

## Unsteady MHD flow of a dusty nanofluid past a vertical stretching surface with non-uniform heat source/sink

C. Sulochana<sup>1</sup>, J. Prakash<sup>2</sup>, N. Sandeep<sup>3#</sup>

<sup>1,3#</sup> Department of Mathematics, Gulbarga University, Gulbarga-585106, India

<sup>2</sup> Department of Mathematics, University of Botswana, Private Bag 0022, Gaborone, Botswana.

Email: [nsreddy.dr@gmail.com](mailto:nsreddy.dr@gmail.com)

**Abstract** - We analyzed the momentum and heat transfer characteristics of unsteady MHD flow of a dusty nanofluid over a vertical stretching surface in presence of volume fraction of dust and nano particles with non uniform heat source/sink. We considered two types of nanofluids namely Ag-water and Cu-water embedded with conducting dust particles. The governing equations are transformed in to nonlinear ordinary differential equations by using similarity transformation and solved numerically using Shooting technique. The effects of non-dimensional governing parameters on velocity and temperature profiles for fluid and dust phases are discussed and presented through graphs. Also, the skin friction coefficient and Nusselt number are discussed and presented for two dusty nanofluids separately in tabular form. Results indicate that an increase in the volume fraction of dust particles enhances the heat transfer in Cu-water nanofluid compared with Ag-water nanofluid and a raise in the volume fraction of nano particles shows uniform heat transfer in both Cu-water and Ag-water nanofluids.

**Keywords** — MHD, Dusty fluid, Nanofluid, Stretching Sheet, Volume fraction, Convection.

Submission: September 10, 2015

Corrected: December 8, 2015

Accepted: January 3, 2016

Doi: 10.12777/ijse.10.1.1-9

[How to cite this article]: Sulochana, C., Prakash, J., Sandeep, N. (2014). Unsteady MHD flow of a dusty nanofluid past a vertical stretching surface with non-uniform heat source/sink, 10(1),1-9. Doi: 10.12777/ijse.10.1.1-9]

### I. INTRODUCTION

Many researchers have investigated the heat and mass transfer characteristics of either dusty or nanofluids through different channels. In this study, we are taking initiative to analyze the momentum and heat transfer characteristics of a dusty nanofluid over a stretching surface by considering volume fraction of dust particles and volume fraction of nano particles. There are tremendous applications for dusty and nanofluids individually in engineering and sciences (Marble, 1970, Wang and Mujumdari, 2008)). Through this initiative, we try to focus on the metals or metallic oxides (mm or micro meters) which give good thermal enhancement by embedding into various nanofluids. (Debnath and Ghosh, 1988) considered dusty fluid flow between two oscillating plates. MHD dusty fluid flow through stretching surface was analyzed by (Chakrabarti and Gupta, 1979). (Datta and Dalal, 1995) discussed heat transfer characteristics of dusty viscous flow over circular pipe. (Bagewadi and Shanharajappa, 2000) analyzed dusty fluid flow over Frenet frame field. Oztop and Abu Nada (2008) discussed natural convective heat transfer through partially heated rectangular enclosures filled with nanofluid. (Ibrahim Saidu et al., 2011) discussed convective heat transfer of dusty viscous fluid by considering volume fraction of dust particles. (Mohan Krishna et al., 2015) discussed the effects of radiation and chemical reaction on MHD convective flow over a permeable stretching surface.

The heat transfer effect on unsteady stretching permeable sheet with combined effect in the presence of thermal radiation and non-uniform heat source/sink is discussed by (Pal, 2011). (Vajravelu et al., 2011) have discussed heat transfer analysis of convective nanofluid through a stretching surface with Ag-water and Cu-water. They concluded that increase in volume fraction of nanoparticles depreciates the velocity and thermal boundary layers. (Hady et al., 2012) analyzed the radiation effect on viscous nanofluid over a nonlinear stretching sheet. (Giresha et al., 2012) discussed heat transfer characteristics of dusty viscous fluid over stretching sheet. (Pal and Mondal., 2012) have studied the effect of non-uniform heat source or sink on MHD mixed convective flow with variable viscosity in the presence of porous medium. (Makinde et al., 2013) analyzed the combined MHD convective heat transfer with buoyancy effects past a Nanofluid over a heated stretching sheet and presented dual solutions by varying buoyancy parameter. (Raju et al. 2015a, 2015b, 2015c) discussed the radiation effect on the flow over a stretching sheet and a flat plate. They extended this work for ferro fluids also. (Sandeep et al., 2014) discussed the aligned magneticfield, radiation and rotation effects on unsteady hydro magnetic free convection flow past an impulsively moving vertical plate. (Sulochana and Sandeep, 2015) discussed the stagnation-point flow and heat transfer behavior of Cu-water nanofluid towards

horizontal and exponentially stretching/shrinking cylinders. Effect of radiation and viscous dissipation on stagnation-point flow of a micropolar fluid over a nonlinearly stretching surface was discussed by (Jayachandra Babu et al., 2015).

Stagnation point flow of an unsteady boundary layer through a shrinking/stretching sheet was discussed by (Bhattacharya, 2013) and presented interesting results on existence of dual solution as well as unique solution and also explained the increase in heat transfer rate causes the unsteadiness parameter. The researchers (Sandeep et al., 2013, Mohan Krishna et al., 2014) discussed the heat transfer characteristics on nanofluids by immersing the high conductivity nano materials in base fluids and they concluded that the effective thermal conductivity of the fluid increases appreciably and consequently enhances the heat transfer characteristics by suspending the high thermal conductivity of nano materials in to the base fluids. (Sheikholeslami et al., 2014) proposed numerical analysis of a heat transfer and magnetic effect on a nanofluid in a rotating surface. (Malyandi et al., 2014) discussed the numerical analysis of a two-dimensional unsteady nanofluid through stretching sheet in the presence of slip condition and showed the increase in heat transfer rate that causes the slip condition. (Rana and Bhargava, 2012) used finite element and finite difference methods for nonlinear stretching sheet problem. (Zaimi et al., 2014) extended the work of (Rana and Bhargava, 2012) and studied heat transfer of steady boundary layer flow of a nano fluid over a stretching/shrinking sheet.

All the references cited above studied either dusty or nanofluid flows through different channels. To our knowledge so far, no any study is done to investigate the momentum and heat transfer characteristics of dusty nanofluid over a vertical stretching sheet by considering volume fraction of the dust and nano particles along with non-uniform heat source/sink. In this work, we studied momentum and heat transfer characteristics of MHD dusty nanofluid over stretching surface by taking volume fraction of dust and nano particles in to account. The governing equations of the flow are solved numerically by using shooting technique. The effect of governing parameters on velocity, temperature, friction factor and Nusselt number are discussed and presented through graphs and tables.

## II. MATHEMATICAL FORMULATION

Consider unsteady two dimensional MHD boundary layer flow of a dusty nanofluid over a semi infinite vertical stretching surface. The stretching sheet is accelerating with non uniform velocity  $U_w(x, t)$ . The flow starts at  $t = 0$  and it is steady at  $t < 0$ . A variable magnetic field  $B$  is applied to the flow as shown in Fig. I. The space and temperature dependent internal heat source/sink (non-uniform heat source/sink) is considered. The dust particles are assumed uniform in size. Spherical shaped nano and dust particles are considered. Number density of dust particles along with the volume fraction of dust and nano particles are taken into account.  $T_w(x, t)$  and  $T_\infty$  are the wall and ambient temperatures respectively.

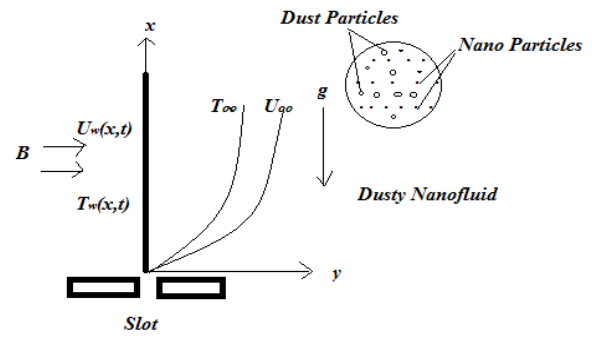


Fig. 1. Physical Model of the problem

Under above assumptions the boundary layer equations of dusty nanofluid can be written in the form

$$\frac{\partial u}{\partial x} + \frac{\partial v}{\partial y} = 0, \quad (1)$$

$$\rho_{nf}(1 - \phi_d) \left( \frac{\partial u}{\partial t} + u \frac{\partial u}{\partial x} + v \frac{\partial u}{\partial y} \right) = (1 - \phi_d) \left[ \mu_{nf} \frac{\partial^2 u}{\partial y^2} + g(\rho\beta)_{nf}(T - T_\infty) \right] + KN(u_p - u) - \sigma B^2 u, \quad (2)$$

$$Nm \left( \frac{\partial u_p}{\partial t} + u_p \frac{\partial u_p}{\partial x} + v_p \frac{\partial u_p}{\partial y} \right) = KN(u - u_p), \quad (3)$$

$$\frac{\partial u_p}{\partial x} + \frac{\partial v_p}{\partial y} = 0, \quad (4)$$

$$(\rho c_p)_{nf} \left( \frac{\partial T}{\partial t} + u \frac{\partial T}{\partial x} + v \frac{\partial T}{\partial y} \right) = k_{nf} \frac{\partial^2 T}{\partial y^2} + q''' \quad (5)$$

With the boundary conditions

$$u = U_w(x, t), v = V_w(t), T = T_w(x, t) \text{ at } y = 0, \\ u \rightarrow 0, u_p \rightarrow 0, v_p \rightarrow v, T \rightarrow T_\infty \text{ as } y \rightarrow \infty, \quad (6)$$

where  $(u, v)$  and  $(u_p, v_p)$  are the velocity components of the fluid and particle phase respectively in  $x, y$  directions,  $\phi_d$  is the volume fraction of the dust particles,  $\rho_{nf}$  and  $\mu_{nf}$  are the nanofluid density and dynamic viscosity respectively,  $\beta_{nf}$  is the thermal expansion of the nanofluid,  $g$  is the acceleration due to gravity,  $K = 6\pi a\mu$  is the stokes resistance (drag coefficient), where  $a$  is the spherical radius of the dust particles,  $\mu$  is the coefficient of viscosity of the fluid particles,  $N$  is the number density of the dust particles,  $m$  is the mass concentration of dust particles,  $\sigma$  is the electrical conductivity,  $B = B_0 / \sqrt{1 - ct}$  is the magnetic field imposed along the  $y - axis$ ,  $(\rho c_p)_{nf}$  is the specific heat capacitance of nanofluid and  $k_{nf}$  is the effective thermal conductivity of nano-fluid,  $q'''$  is non uniform heat source/sink and  $t$  refers to the time,  $U_w(x, t) = ax / 1 - ct$  is stretching sheet velocity,  $a$  is the initial stretching rate,  $c$  is the positive constant which measures the unsteadiness.  $V_w(t) = v_0 / \sqrt{1 - ct}$  is the mass transfer velocity. We have  $a / 1 - ct$  initial stretching rate increasing with time. The space and temperature dependent heat generation/absorption (non uniform heat source/sink)  $q'''$  is defined as

$$q''' = \left( \frac{k_f U_w(x, t)}{x v_f} \right) (A^* (T_w - T_\infty) f' + B^* (T - T_\infty)), \quad (7)$$

where  $A^*$  and  $B^*$  are parameters of the space and temperature dependent internal heat generation/absorption. The positive and negative values of  $A^*$  and  $B^*$  represents heat generation and absorption respectively. The nanofluid constants are given by

$$\begin{aligned} (\rho\beta)_{nf} &= (1 - \phi)(\rho\beta)_f + \phi(\rho\beta)_s, \\ (\rho c_p)_{nf} &= (1 - \phi)(\rho c_p)_f + \phi(\rho c_p)_s, \\ \frac{k_{nf}}{k_f} &= \frac{(k_s + 2k_f) - 2\phi(k_f - k_s)}{(k_s + 2k_f) + \phi(k_f - k_s)}, \\ \mu_{nf} &= \frac{\mu_f}{(1 - \phi)^{2.5}}, \quad \rho_{nf} = (1 - \phi)\rho_f + \phi\rho_s, \end{aligned} \quad (8)$$

Where  $\phi$  is the volume fraction of the nano particles. The subscripts  $f$  and  $s$  refer to fluid and solid properties respectively.

Using the following similarity transformations, the governing equations are given from (1) to (5) subject to the boundary condition (6) into coupled non linear ordinary differential equations,

$$\begin{aligned} \eta &= \left( \frac{a}{v_f(1 - ct)} \right)^{1/2} y, \quad \psi(x, y) = \left( \frac{v_f a}{1 - ct} \right)^{1/2} x f(\eta), \\ \psi(x, y) &= \left( \frac{v_f a}{1 - ct} \right)^{1/2} x F(\eta), \quad T = T_w = T_\infty + \frac{bx}{(1 - ct)^2} \theta(\eta), \\ \theta(\eta) &= \frac{T - T_\infty}{T_w - T_\infty}, \end{aligned} \quad (9)$$

where the stream function  $\psi$  identically satisfies the continuity equations (1) and (4) with

$$\begin{aligned} u &= \frac{ax}{1 - ct} f'(\eta), \quad v = -\sqrt{\frac{v_f a}{1 - ct}} f(\eta), \\ u_p &= \frac{ax}{1 - ct} F'(\eta), \quad v_p = -\sqrt{\frac{v_f a}{1 - ct}} F(\eta), \end{aligned} \quad (10)$$

Using equations (8) to (10), the equations (2), (3), (5), (6) along with (7) reduces to

$$\left. \begin{aligned} \frac{(1 - \phi_d)}{(1 - \phi)^{2.5}} f''' - (1 - \phi_d)(1 - \phi + \phi(\rho_s / \rho_f)) \\ \left( f'^2 - ff'' + Af' + \frac{A\eta}{2} f'' \right) - Mf' + \alpha\beta(F' - f') \\ + (1 - \phi + \phi((\rho\beta)_s / (\rho\beta)_f)) \lambda \theta = 0 \end{aligned} \right\} \quad (11)$$

$$FF'' - AF' - \frac{A\eta}{2} F'' - F'^2 - \beta(f' - F') = 0 \quad (12)$$

$$\left. \begin{aligned} \frac{1}{Pr} \frac{k_{nf} / k_f}{1 - \phi + \phi((\rho c_p)_s / (\rho c_p)_f)} \theta'' \\ - \left( A\theta + \frac{A\eta}{2} \theta' + \theta f' - f \theta' \right) \\ + \frac{1}{Pr} \frac{1}{1 - \phi + \phi((\rho c_p)_s / (\rho c_p)_f)} (A^* f' + B^* \theta) = 0 \end{aligned} \right\} \quad (13)$$

Subject to boundary conditions

$$\begin{aligned} f(\eta) = f_w, \quad f'(\eta) = 1, \quad \theta(\eta) = 1 \quad \text{at } \eta = 0 \\ f'(\eta) = 0, \quad F'(\eta) = 0, \quad F(\eta) = -f(\eta), \\ \theta(\eta) = 0 \quad \text{as } \eta \rightarrow \infty \end{aligned} \quad (14)$$

where primes denotes differentiation with respect to  $\eta$ ,  $A = c / a$  is the unsteadiness parameter,  $M = \sigma B_0^2 / \rho_f a$  is the magnetic field parameter,  $\alpha = Nm / \rho_f$  is the mass concentration of the dust particles,  $\beta = (1 - ct) / a\tau_v$  is the fluid particle interaction parameter,  $\tau_v = m / K$  is the relaxation time of the dust particles,  $\lambda = g\beta_f b / a^2$  is the thermal buoyancy parameter,  $Pr$  is the Prandtl number,  $f_w = v_0 / \sqrt{bc}$  is suction parameter,  $A^*$  and  $B^*$  are the heat source/sink parameters.

For engineering interest the local skin friction coefficient  $C_f$  and Nusselt number  $Nu_x$  are given by

$$C_f Re_x^{1/2} = (1 - \phi)^{-1/2} f''(0) \quad (15)$$

$$Nu_x Re_x^{-1/2} = -(k_{nf} / k_f) \theta'(0) \quad (16)$$

where  $Re_x = U_w x / v_f$  is the local Reynolds number.

### III. RESULT AND DISCUSSION

The coupled ordinary differential equations (11) to (13) subject to the boundary conditions (14) are solved numerically using shooting technique. The results obtained shows the influences of the non dimensional governing parameters, namely volume fraction of dust particles  $\phi_d$ , volume fraction of nano particles  $\phi$ , unsteadiness parameter  $A$ , mass concentration of the dust particles  $\alpha$ , fluid particle interaction parameter  $\beta$ , magneticfield parameter  $M$ , thermal buoyancy parameter  $\lambda$ , heat source/sink parameters  $A^*$  and  $B^*$  on velocity and temperature profiles for fluid and dust phase for Ag-water and Cu-water dusty nanofluids was discussed and presented through graphs. Also, friction factor and Nusselt numbers are discussed and presented through tables. For numerical results, we considered  $A = \alpha = \beta = 0.5, Pr = 6.2, \eta = 5, \lambda = 0.2, M = 1, A^* = B^* = 0.2, \phi = \phi_d = 0.1$ . These values kept as common in entire study except the varied values as shown in figures. The thermo-physical properties of water, Copper, Silver are displayed in Table 1.

**Table 1.** Thermo-physical properties of base fluid and different nano particles.

|       | $\rho(Kg m^{-3})$ | $c_p(J Kg^{-1} K^{-1})$ | $k(Wm^{-1} K^{-1})$ | $\beta \times 10^{-5} K^{-1}$ |
|-------|-------------------|-------------------------|---------------------|-------------------------------|
| Water | 997.1             | 4179                    | 0.613               | 21                            |
| Cu    | 8933              | 385                     | 401                 | 1.67                          |
| Ag    | 10500             | 235                     | 429                 | 1.89                          |

Figs.1 and 2 depict the variation in velocity profiles of nanofluid and dust phases along with temperature profiles for both Ag-water and Cu-water dusty nanofluids for different values of volume fraction of dust particles. It is evident from Fig.1 that increase in volume fraction of dust particles depreciate the velocity profiles of the fluid and dust phases for both Ag-water and Cu-water dusty nano fluids. It is observed that increases in volume fraction of dust particles affects more on Cu-water fluid compared to Ag-water fluid. This may happen due to the reason that an increase in the concentration of Cu-water fluid effectively reduces the boundary layer thickness of velocity profiles compared to Ag-water fluid. From Fig. 2 it is observed that an increase in the volume fraction of dust particles enhances the temperature profiles of

both dusty nano fluids. It is interesting to observe that an increase in dust particle volume fraction effectively helps to enhance the temperature profiles of Cu-water fluid compared to Ag-water fluid. Also, an increase in dust particle volume fraction reduces the heat transfer rate for both fluids but this reduction rate is high in Cu-water fluid compared to Ag-water fluid as displayed in Tables 2 and 3.

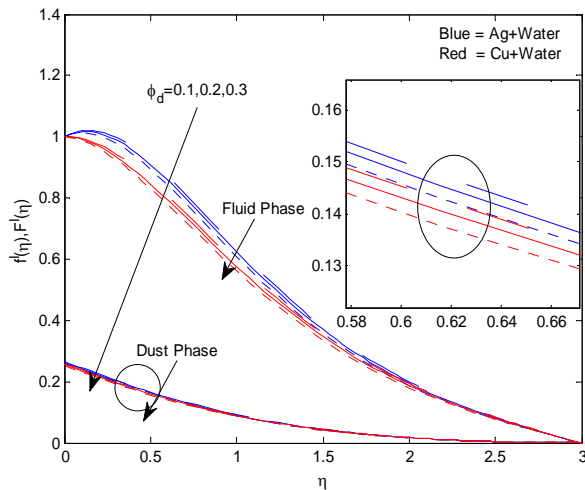


Figure 1. Variation in velocity profiles

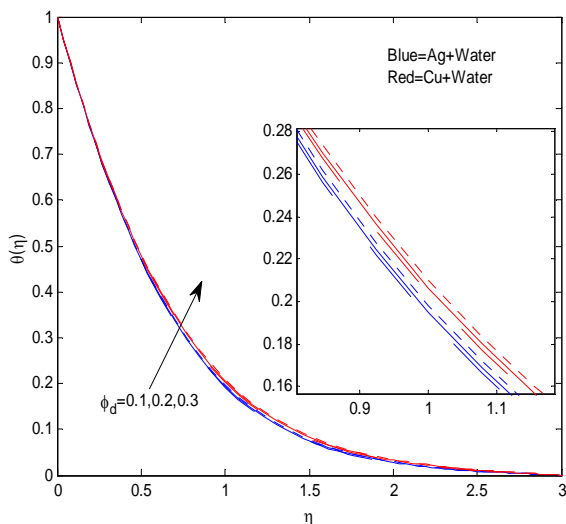


Figure 2. Variation in temperature profiles

Figs.3 and 4 show the variation in velocity profiles of nanofluid and dust phases along with temperature profiles for both Ag-water and Cu-water dusty nanofluids for different values of volume fraction of nano particles. It is interesting to observe that an increase in volume fraction of the nano particles enhance the velocity and temperature profiles of both Ag-water and Cu-water dusty nano fluids uniformly along with velocity and thermal boundary layer thickness. It is evident from figures that the velocity profiles of the dust and nanofluid phases display up to  $\eta_{\infty} = 2$  and  $\eta_{\infty} \geq 3$  level. But we can notice the reduced velocity boundary layer thickness due to increase in volume fraction of dust particles from Fig.1 (i. e. the velocity profiles displays only up to  $\eta_{\infty} = 1.2$  and  $\eta_{\infty} = 2.3$  in Fig.1 for dust and fluid phases). Similarly, we can observe the enhancement in the thermal boundary layer thickness in Fig. 4 compared with Fig. 2. From Tables 2 and 3 we have observed a gradual depreciation

in heat transfer rate in both fluids by an increase in volume fraction of the nano particles. This reduction is significantly high while compared with volume fraction enhancement of dust particles.

Figs. 5 and 6 illustrates the variation in velocity profiles of nanofluid and dust phases of Ag-water and Cu-water dusty nanofluids along with temperature profiles for different values of unsteadiness parameter ( $A$ ). It is clear from Fig. 5 that an increase in unsteadiness parameter increases the velocity and temperature profiles of the nanofluid phase. But in dust phase initially it takes opposite action to the fluid phase, again at  $\eta = 1.3$  level it takes reverse action and follows the fluid phase, which respectively indicates the square and elliptical boxes for detailed observations. Physically this means that an increase in acceleration helps to improve the velocity of the fluid phase but in particle phase it takes minimum time called peak time to follow the velocity profiles. An increased unsteadiness improves the interaction between the particle and fluid phase which indirectly helps to develop the thermal conductivity. Due to this reason we have seen enhancement in temperature profiles also.

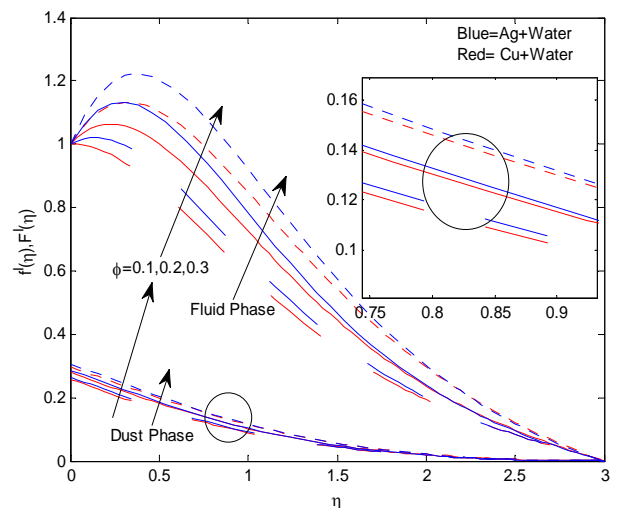


Figure 3. Variation in velocity profiles

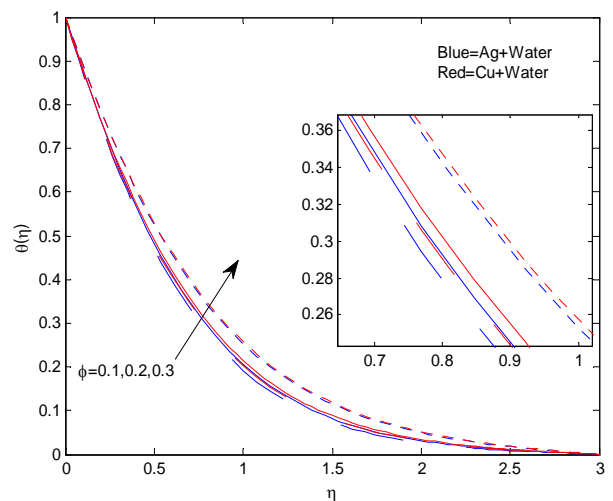


Figure 4. Variation in temperature profiles

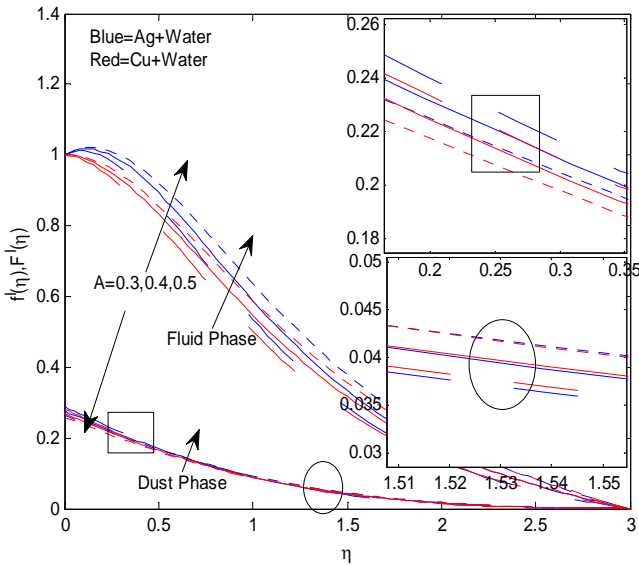


Figure 5. Variation in velocity profiles

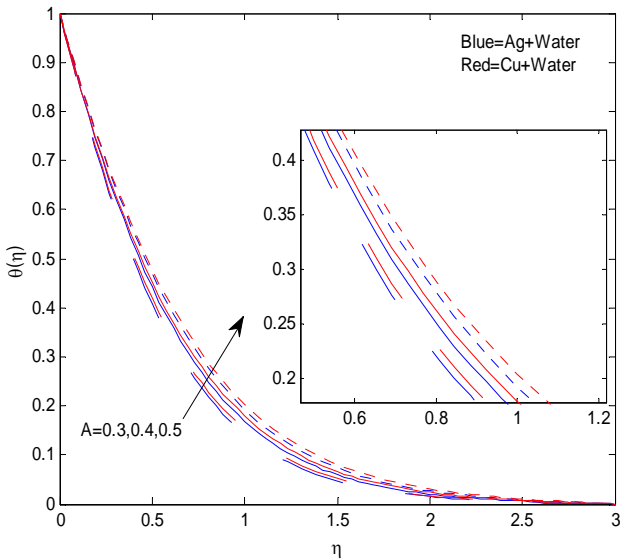


Figure 6. Variation in temperature profiles

Figs.7 and 8 display the variation in velocity profiles of nanofluid and dust phases of Ag-water and Cu-water dusty nanofluids along with temperature profiles for different values of fluid particle interaction parameter ( $\beta$ ). It is evident from Fig.7 that an increase in fluid particle interaction parameter increases the velocity profiles of the particle phase and decreases the velocity profiles of the nanofluid phase for both fluids. It is due to this fact that the interaction between the fluid and particles is high then particles generate the opposite force to the flow. This force declines the velocity profiles of the fluid or simply we can say that the particle phase slows down the fluid velocity until it reaches the fluid velocity. During these time interval particle phase continuously dominates the fluid phase till both are having equal in velocities. From Fig.8 we noticed an enhancement in temperature profiles by an increase in fluid particle interaction. This agrees the physical property that the increase in interaction between the fluid and particles improves the thermal conductivity which helps to develop the temperature profiles.

Figs.9 and 10 represent the variation in velocity profiles of nanofluid and dust phases of Ag-water and Cu-water dusty nanofluids along with temperature profiles for different values of mass concentrations of dust particles ( $\alpha$ ). It is noticed that an increase in mass concentration of the dust particles depreciates the velocity profiles of the fluid as well as dust phases and it takes reverse action in case of temperature profiles. Generally an increase in mass concentration of dust particles means the increase in the number density of the dust particles. It is expected that if number density of the dust particles is more then it declines the velocity profiles and enhances the thermal boundary layer thickness. This is in agreement with the general phenomenon.

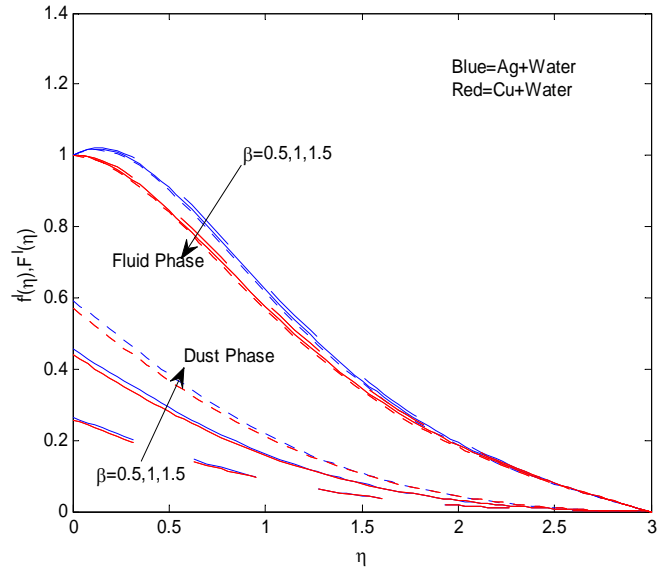


Figure 7. Variation in velocity profiles

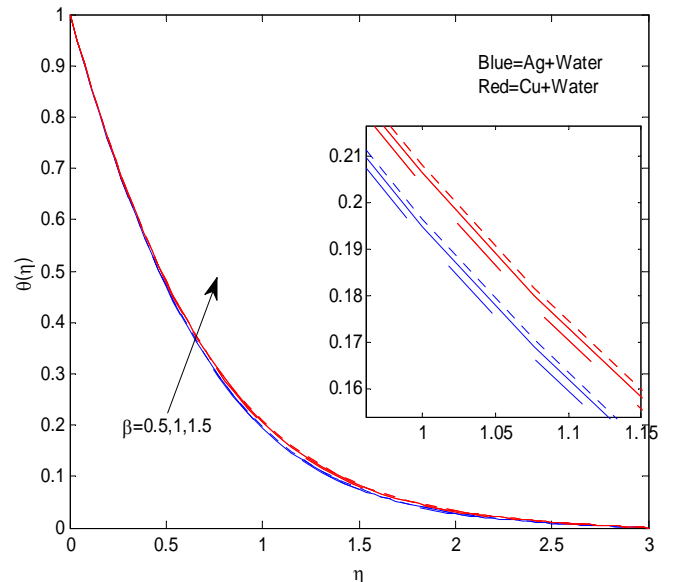


Figure 8. Variation in temperature profiles

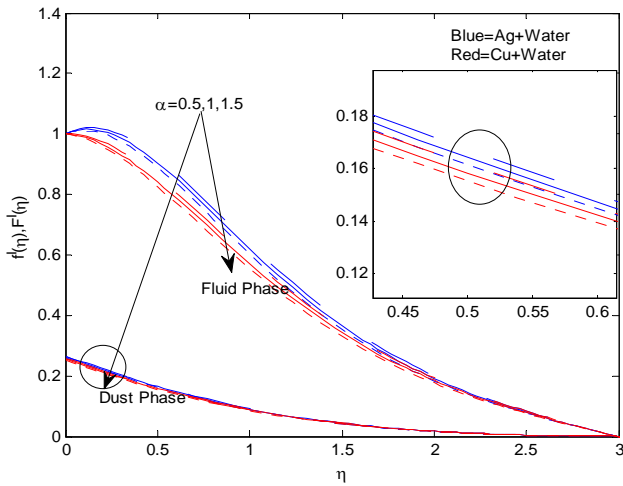


Figure 9. Variation in velocity profiles

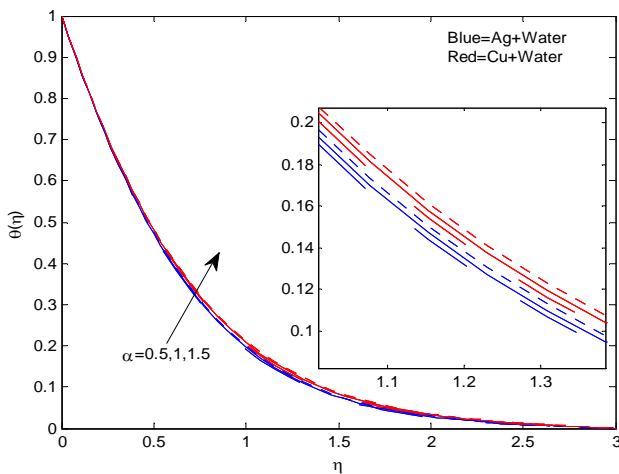


Figure 10. Variation in temperature profiles

Figs.11 and 12 reveal the variation in velocity profiles of nanofluid and dust phases of Ag-water and Cu-water dusty nanofluids along with temperature profiles for different values of magnetic field parameter ( $M$ ). It is observed from Fig.11 that an increase in magnetic field parameter depreciates the velocity profiles for both fluid and dust phases. This effect is high on dust phase compared to fluid phase. This is due to the fact that an increase in magnetic field generates the opposite force to the flow, called Lorentz force. This force slows down the velocity profiles and improves the thermal boundary layer.

Figs.13 and 14 show the variation in velocity profiles of nanofluid and dust phases of Ag-water and Cu-water dusty nanofluids for different values of non uniform heat source/sink parameters. It is clear from figures that an increase in heat source/sink parameters enhances the velocity profiles of both fluid and dust phases. The reason behind this is positive and negative values of  $A^*$  and  $B^*$  respectively acts like heat generation and absorption. Here for positive values of  $A^*$  and  $B^*$ , we have observed hike in velocity profiles. That is  $A^*$  and  $B^*$  act like heat generators which help to enhance the thermal boundary layer thickness along with velocity boundary layer. This enhancement in thermal boundary layer improves the temperature profiles as displayed in Figs. 15 and 16. It is evident to conclude that for lesser values of  $A^*$  and  $B^*$  we have observed fall in temperature,

which reveals that negative values of  $A^*$  and  $B^*$  act like heat absorption parameters and positive values as heat generators.

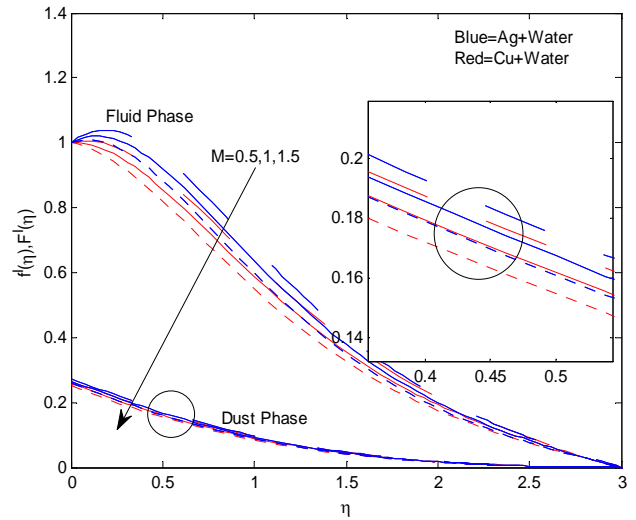


Figure 11. Variation in velocity profiles

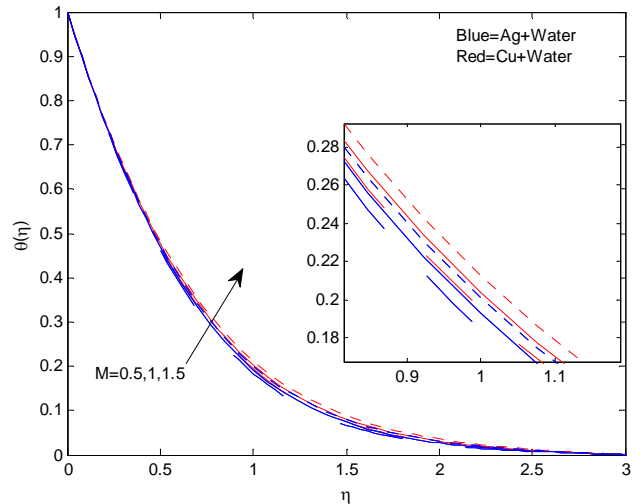


Figure 12. Variation in temperature profiles

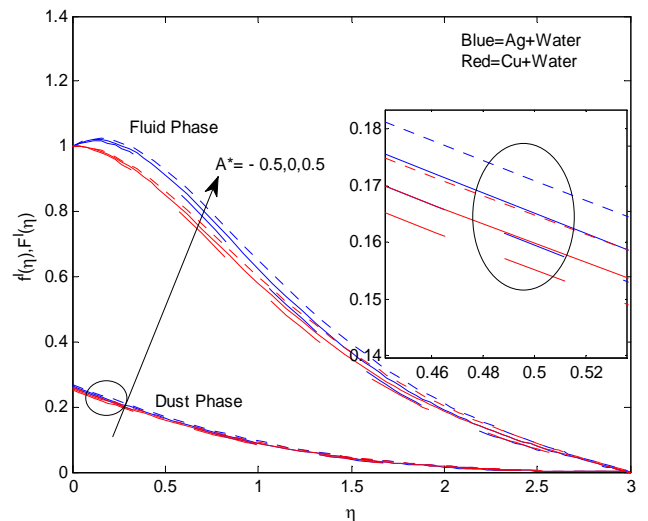


Figure 13. Variation in velocity profiles

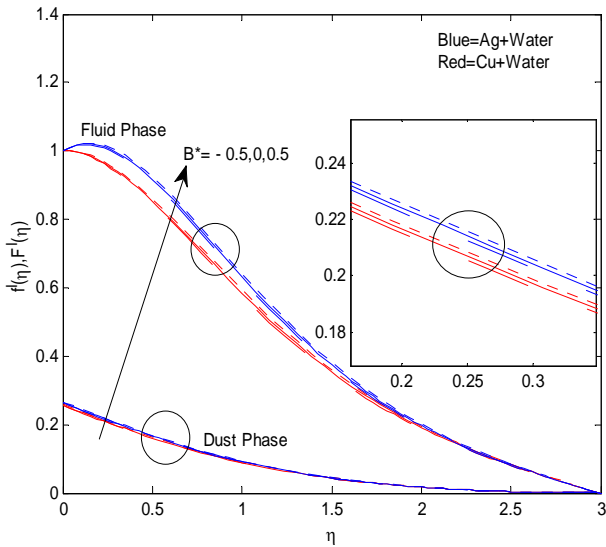


Figure 14. Variation in velocity profiles

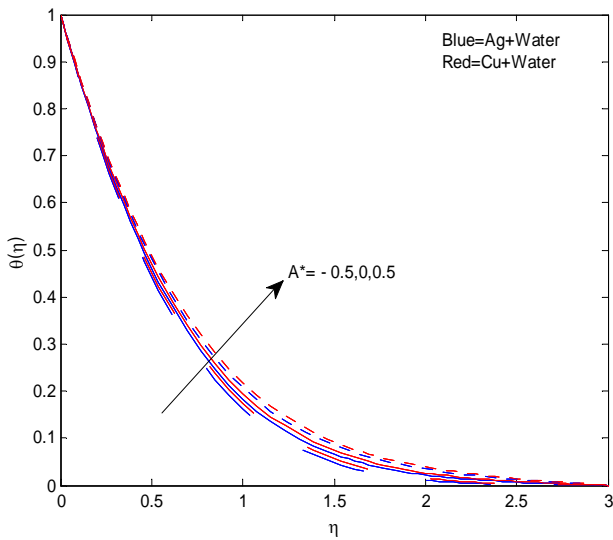


Figure 15. Variation in temperature profiles

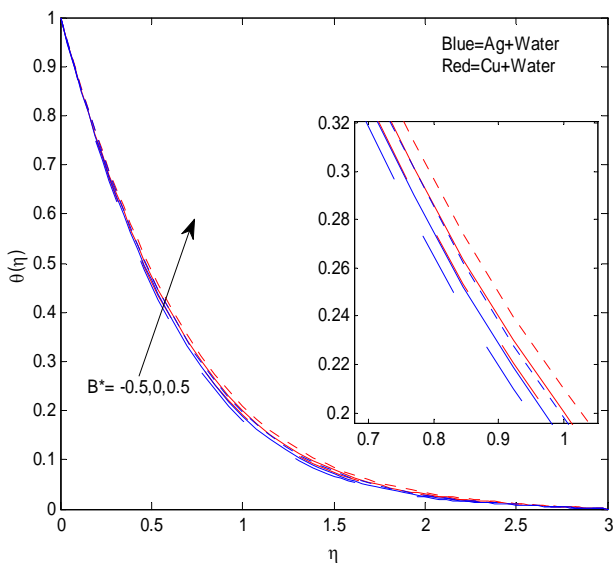


Figure 16. Variation in temperature profiles

Figs. 17 depicts the variation in velocity profiles of nanofluid and dust phases of Ag-water and Cu-water dusty nanofluids along with temperature profiles for different values of thermal buoyancy parameter ( $\lambda$ ). It is evident from Fig.17 that an increase in thermal buoyancy parameter enhances the velocity profiles of both nanofluid and dust phases. Generally, buoyancy parameter is the ratio of the buoyancy to the viscous forces. This will accelerates the fluid and works as a pressure gradient. So, the velocity and boundary layer thickness enhances by hike in buoyancy parameter. From Tables 2 and 3, we noticed that an increase in thermal buoyancy parameter increases the heat transfer rate of both dusty nanofluids. But this rate of heat transfer is significantly high in Ag-water dusty nanofluid compared with Cu-water dusty nanofluid.

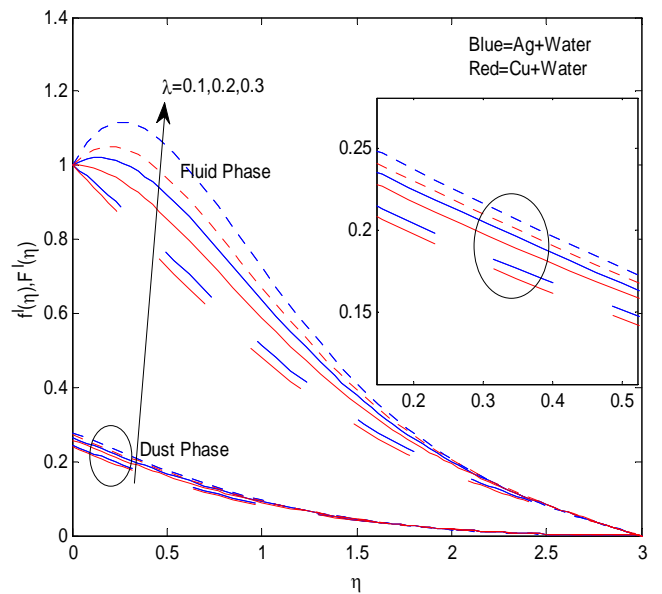


Figure 17. Variation in velocity profiles

Tables 2 and 3 respectively display the effect of governing parameters on friction factor and local Nusselt number for both Cu-water and Ag-water dusty nanofluids. It is evident from the table that increases in volume fraction of dust and nano particles, mass concentration of dust particles, fluid particle interaction parameter, magneticfield parameter, unsteadiness parameter and non-uniform heat source/sink parameters depreciates the heat transfer rate for both dusty nanofluids. But by an increase in the thermal buoyancy parameter, we noticed that an increase in the Nusselt number. The increase in volume fraction of dust particles, mass concentration of dust particles, fluid particle interaction parameter and magneticfield parameter reduces the coefficient of skin friction. But an increase in volume fraction of nano particles, thermal buoyancy parameter, unsteadiness parameter and heat source/sink parameters increase the friction factor.

Table 2. Variation in  $f''(0)$  and  $-\theta'(0)$  for Cu-water dusty nanofluid, when  $Pr = 6.2$

| $\phi_d$ | $\phi$ | $\alpha$ | $\beta$ | $\lambda$ | $M$ | $A$ | $A^*$ | $f''(0)$  | $-\theta'(0)$ |
|----------|--------|----------|---------|-----------|-----|-----|-------|-----------|---------------|
| 0.1      |        |          |         |           |     |     |       | 0.034082  | 1.327773      |
| 0.2      |        |          |         |           |     |     |       | -0.002795 | 1.325129      |
| 0.3      |        |          |         |           |     |     |       | -0.049464 | 1.321801      |
|          | 0.1    |          |         |           |     |     |       | 0.034082  | 1.327773      |
|          | 0.2    |          |         |           |     |     |       | 0.601320  | 1.267917      |
|          | 0.3    |          |         |           |     |     |       | 0.904194  | 1.146310      |
|          |        | 0.5      |         |           |     |     |       | 0.034082  | 1.327773      |
|          |        | 1.0      |         |           |     |     |       | -0.014185 | 1.324256      |
|          |        | 1.5      |         |           |     |     |       | -0.061689 | 1.320821      |
|          |        |          | 0.5     |           |     |     |       | 0.034082  | 1.327773      |
|          |        |          | 1.0     |           |     |     |       | 0.005323  | 1.325557      |
|          |        |          | 1.5     |           |     |     |       | -0.011335 | 1.324181      |
|          |        |          |         | 0.1       |     |     |       | -0.514025 | 1.293134      |
|          |        |          |         | 0.2       |     |     |       | 0.034082  | 1.327773      |
|          |        |          |         | 0.3       |     |     |       | 0.557266  | 1.359169      |
|          |        |          |         |           | 0.5 |     |       | 0.161422  | 1.336954      |
|          |        |          |         |           | 1.0 |     |       | 0.034082  | 1.327773      |
|          |        |          |         |           | 1.5 |     |       | -0.087254 | 1.319147      |
|          |        |          |         |           |     | 0.3 |       | -0.039763 | 1.546697      |
|          |        |          |         |           |     | 0.4 |       | 0.007404  | 1.421490      |
|          |        |          |         |           |     | 0.5 |       | 0.034082  | 1.327773      |
|          |        |          |         |           |     |     | -0.5  | 0.006449  | 1.401540      |
|          |        |          |         |           |     |     | 0     | 0.026101  | 1.348924      |
|          |        |          |         |           |     |     | 0.5   | 0.046183  | 1.295932      |

Table 3 Variation in  $f''(0)$  and  $-\theta'(0)$  for Ag-water dusty nanofluid, when  $Pr = 6.2$

| $\phi_d$ | $\phi$ | $\alpha$ | $\beta$ | $\lambda$ | $M$ | $A$ | $A^*$ | $f''(0)$  | $-\theta'(0)$ |
|----------|--------|----------|---------|-----------|-----|-----|-------|-----------|---------------|
| 0.1      |        |          |         |           |     |     |       | 0.325734  | 1.339947      |
| 0.2      |        |          |         |           |     |     |       | 0.289492  | 1.337343      |
| 0.3      |        |          |         |           |     |     |       | 0.243561  | 1.334059      |
|          | 0.1    |          |         |           |     |     |       | 0.325734  | 1.339947      |
|          | 0.2    |          |         |           |     |     |       | 0.994930  | 1.278772      |
|          | 0.3    |          |         |           |     |     |       | 1.340082  | 1.148095      |
|          |        | 0.5      |         |           |     |     |       | 0.325734  | 1.339947      |
|          |        | 1.0      |         |           |     |     |       | 0.278273  | 1.336471      |
|          |        | 1.5      |         |           |     |     |       | 0.231513  | 1.333068      |
|          |        |          | 0.5     |           |     |     |       | 0.325734  | 1.339947      |
|          |        |          | 1.0     |           |     |     |       | 0.297642  | 1.337744      |
|          |        |          | 1.5     |           |     |     |       | 0.281797  | 1.336380      |
|          |        |          |         | 0.1       |     |     |       | -0.362379 | 1.297162      |
|          |        |          |         | 0.2       |     |     |       | 0.325734  | 1.339947      |
|          |        |          |         | 0.3       |     |     |       | 0.979416  | 1.378160      |
|          |        |          |         |           | 0.5 |     |       | 0.450468  | 1.348942      |
|          |        |          |         |           | 1.0 |     |       | 0.325734  | 1.339947      |
|          |        |          |         |           | 1.5 |     |       | 0.206314  | 1.331440      |
|          |        |          |         |           |     | 0.3 |       | 0.269832  | 1.564334      |
|          |        |          |         |           |     | 0.4 |       | 0.309398  | 1.436512      |
|          |        |          |         |           |     | 0.5 |       | 0.325734  | 1.339947      |
|          |        |          |         |           |     |     | -0.5  | 0.290873  | 1.416663      |
|          |        |          |         |           |     |     | 0     | 0.315648  | 1.361962      |
|          |        |          |         |           |     |     | 0.5   | 0.341052  | 1.306774      |

#### IV. CONCLUSIONS

This paper presents an unsteady MHD flow of a dusty nanofluid over a vertical stretching surface in the presence of volume fraction of dust and nano particles with non uniform heat source/sink. The conclusions of the present study are as follows:

- Embedding the dust particles in nanofluids leads to enhance the temperature profiles of the fluid.
- An increase in the volume fraction of dust particles improves the thermal conductivity of Cu-water nanofluid effectively while compared with Ag-water.
- The thermal buoyancy parameter helps to increase the heat transfer rate for both Cu-water and Ag-water dusty nanofluids.
- Unsteadiness parameter have tendency to improve the heat temperature profiles along with friction factor for both dusty nanofluids.
- Fluid particle interaction parameter, mass concentration of dust particles and magneticfield parameter improve the temperature profiles but depreciates the friction factor.

#### ACKNOWLEDGMENT

Authors from Gulbarga University acknowledge the UGC for financial support under the UGC Dr. D. S. Kothari Post-Doctoral Fellowship Scheme (No.F.4-2/2006 (BSR)/MA/13-14/0026).

#### REFERENCES

Begewadi, C.S. and Shantharajappa, A.N. 2000. A study of unsteady dusty gas flow in Frenet Frame field, Ind. J. Pure and App. Math., 31:1405-1420.

Bhattacharyya, K. 2013. Heat transfer analysis in unsteady boundary layer stagnation-point flow towards a shrinking/stretching sheet. Ains Shams Engineering Journal, 4(2):259-264.

Chakrabarti, A. and Gupta, A. S. 1979. Hydromagnetic flow and heat transfer over a stretching sheet. Quarterly of Applied Mathematics., 37:73-98.

Datta, N., and Dalal, D. C. 1995. Pulsatile flow of heat transfer of a dusty fluid through an infinitely long annular pipe. Int. J. Multiphase flow, 21(3):515-528.

Debnath, L., Ghosh, A.K. 1988. On unsteady hydromagnetic flows of a dusty fluid between two oscillating plates. Appl.Sci.Res., 45:353-356.

Giresha, B.J., Roopa, G.S., Lokesh, H.J., and Bagewadi, C.S. 2012. MHD flow and heat transfer of a dusty fluid over a stretching sheet. Int.J.physical and mathematical sciences, 3(1):171-180.

Hady, F.M., Ibrahim, F.S., Abdel-Gaied, S.M., and Eid, M.R. 2012. Radiation effect on viscous flow of a nanofluid and heat transfer over a nonlinearly stretching sheet, Nanoscale Research Letters, 7:299-310.

Ibrahim Saidu, Waziri, M .M., Abubakar Roko and Hamisu, M. 2010. MHD effects on convective flow of dusty viscous fluid with volume fraction of dust particles. ARPN J of Eng and applied sciences, 5:86-91.

Jayachandra Babu, M., Radha Gupta, Sandeep. N. 2015. Effect of radiation and viscous dissipation on stagnation-point flow of a micropolar fluid over a nonlinearly stretching surface with suction/injection. Journal of Basic and Applied Research International, 7(2):73-82.

Makinde, O.D., Khan, W.A., Khan, Z. H. 2013. Buoyancy effects on MHD stagnation point flow and heat transfer of a Nanofluid past a convectively heated stretching/shrinking sheet. Int.J.Heat and Mass transfer, 62:526-533.

Malyand, A., Hedayati, F., Ganji, D. D. 2014. Slip effects on unsteady stagnation point flow of Nanofluid over a stretching sheet. J. Power Technology, 253:377-384.

Marble, F. E. 1970. Dynamics of dusty gases. Annual review of fluid mech., 2:397-446. DOI: 10.1146/annurev.fl.02.010170.002145.

Mohankrishna, P., Sugunamma, V., Sandeep, N. 2014. Radiation and magneticfield effects on unsteady natural convection flow of a nanofluid past an infinite vertical plate with heat source.Chemical and Process Engineering Research, 25:39-52.

Mohankrishna, P., Sandeep, N, Sugunamma, V. 2015. Effects of radiation and chemical reaction on MHD convective flow over a permeable stretching surface with suction and heat generation. Walaliak Journal of Science and Technology, 12(9): 831-847.

Oztop, H.F., Abu-Nada, E. 2008. Numerical study of natural convection in partially heated rectangular enclosures filled with nanofluids. Int. J. of Heat Fluid Flow, 29:1326-1336.

Pal, D. 2011. Combined effects of non-uniform heat source/sink and thermal radiation on heat transfer over an unsteady stretching permeable surface. J. Communications in Nonlinear Science and Numerical Simulation, 16 (4):1890-1904.

Pal, D., Mondal, H. 2012. MHD non-Darcy mixed convective diffusion species over a stretching sheet embedded in a porous medium with non-uniform heat source/sink, variable viscosity and solet effect. J. Communications in Nonlinear Science and Numerical Simulation, 17(2):672-684.

Raju, C.S.K., Jayachandra Babu, M, Sandeep, N, Sugunamma, V., Ramanareddy, J.V. 2015a. Radiation and solet effects of MHD nanofluid flow over a moving vertical plate in porous medium. Chemical and Process Engineering Research 30:9-23;

Raju, C.S.K, Sandeep, N, Sulochana, C., Sugunamma, V., Jayachandrababu, M. 2015b. Radiation, inclined magnetic field and cross-diffusion effects on flow over a stretching surface. Journal of the Nigerian Mathematical Society, 34:169-180.

Raju, C.S.K, Sandeep, N, Sulochana, C., Sugunamma, V. 2015c. Effects of aligned magneticfield and radiation on the flow of ferrofluids over a flat plate with non-uniform heat source/sink. Internat. J. Sci. Eng., Vol. 8(2)2015:151-158,

Rana, P. and Bhargava, R. 2012. Flow and heat transfer of a nanofluid over a nonlinearly stretching sheet: a numerical study. Commun. Nonlinear Sci. Numer. Simulation, 17: 212-226.

Sandeep, N., Sugunamma, V., Mohankrishna, P. 2013. Effects of radiation on an unsteady natural convective flow of a EG-Nimonic 80a nanofluid past an infinite vertical plate. Advances in Physics Theories and Applications, 23:36-43.

Sandeep, N, Sugunamma, V, Mohan Krishna, P. 2014. Aligned Magneticfield, Radiation and Rotation Effects on Unsteady Hydro Magnetic Free Convection Flow Past an Impulsively Moving Vertical Plate in a Porous Medium. Int J Eng Mathematics ID 565162, <http://dx.doi.org/10.1155/2014/565162>.

Sheikholeslami, M., Hatami, M., Ganji, D.D. 2014. Nanofluid flow and heat transfer in a rotating system in the presence of a magneticfield. J. Molecular Liquids, 190:112-120.

Sulochana, C., and Sandeep, N. 2015. Stagnation-point flow and heat transfer behavior of Cu- water nanofluid towards horizontal and exponentially stretching/shrinking cylinders. Applied Nanoscience 5 (2015) (In Press).

Vajravelu, K., K. V. Prasad, JinhoLee, Changhoon Lee, Pop, I., Van Gorder, R. A. (2011). Convective heat transfer in the flow of viscous Ag-water and Cu-water nanofluids over a stretching surface. Int. J. Thermal Sciences, 50 (5):843-851.

Wang, X. Q., and Mujumdari, A. 2008. A review on nanofluids-Part II experiments and applications. Brazilian Journal of Chemical Engineering, 25(4):631-648.

Zaimi, K., Ishak, I., and Pop, I. 2014. Boundary layer flow and heat transfer over a nonlinearly permeable stretching/shrinking sheet in a nanofluid, Plos One 4: 4404 | DOI: 10.1038/srep04404.